Biochimica et Biophysica Acta, 984 (1989) 281–288
Elsevier

BBAMEM 74555

A method to distinguish between pore and carrier kinetics applied to urea transport across the erythrocyte membrane

Lenore W. Yousef and Robert I. Macey

Biology Department, California State University, Fresno and Department of Physiology-Anatomy, University of California, Berkeley (U.S.A.)

(Received 2 June 1989)

Key words: Urea; Erythrocyte; Channel; Carrier; Kinetics; Permeability

Permeability coefficients (P) measured at various penetrant concentrations (C) by the perturbation method can be plotted to distinguish simple diffusion, simple pore kinetics and simple carrier kinetics as follows: for simple diffusion, $1/P$ = constant; for a simple pore, $1/P = 1/P_o + 1/P_o[1/K_{in} + 1/K_o]C$; for a simple carrier, $1/P = 1/P_o + 1/P_o[1/K_{in} + 1/K_o]C + 1/P_o[1/(K_3K_4)]C^2$ where P_o is the maximal permeability at zero penetrant concentration and the K's are combinations of kinetic constants defining each of the transport steps. (K_{in} and K_o are the half-saturation constant for zero-trans efflux and influx, respectively; K_3 is the half-saturation cosntant for equilibrium exchange, and K_4 is related to the mobility of the free carrier.) In human erythrocytes, permeability coefficients for diethylene glycol were constant suggesting simple diffusion. For glucose, a plot of $1/P$ versus concentration was nonlinear indicating carrier kinetics. Plots of $1/P$ versus penetrant concentrations gave straight lines with positive slopes for urea in human and bovine erythrocytes and for methylurea in human red cells, indicating these penetrants follow simple pore kinetics or simple carrier kinetics in which K_4 is very large.

Introduction

Although urea moves across the human red blood cell membrane by some type of mediated transport system [1–3], very little is known of the actual mechanism. Measurements useful for distinguishing between the 'simple pore (channel)' and 'simple carrier' models, as trans acceleration and counter-transport, are more difficult for urea than for slower penetrants since, for urea, both water and solute permeation is very rapid. Thus, cell volumes and internal urea concentrations change rapidly during the time course of tracer measurements. Here, we base our work on the kinetic definitions of the simple pore and the simple carrier models given by Lieb [5] and Stein [6,7], and introduce a relatively simple way to distinguish between pore and carrier as follows.

Permeability coefficients are measured at various penetrant concentrations with the perturbation method [4]. A linear dependence of the inverse of permeability coefficients on penetrant concentration signifies a simple pore and a non-linear dependence a simple carrier. For urea, a simple pore fits the data much better than the simple carrier, although more complex kinetic models cannot be ruled out.

Materials and Methods

Distinguishing among simple diffusion, the simple pore and the simple carrier

If the concentrations of passively permeating nonelectrolyte on the outer and inner surfaces of a membrane are given by C_o and C_{in}, then, we define the permeability, P, as the ratio of the net molar flux, J, to the concentration gradient, i.e.

$$P = \frac{J}{(C_o - C_{in})} \tag{1}$$

In general, P is a function of C_{in} and C_o. P takes different forms depending on whether the permeation takes place via simple diffusion, a simple pore, or a simple carrier [5–8] as follows:

$$P = P_o = \text{constant} \qquad \text{(diffusion)} \tag{2}$$

$$P = \frac{P_o}{1 + \frac{C_o}{K_o} + \frac{C_{in}}{K_{in}}} \qquad \text{(pore)} \tag{3}$$

$$P = \frac{P_o}{1 + \frac{C_o}{K_o} + \frac{C_{in}}{K_{in}} + \frac{C_oC_{in}}{K_3K_4}} \qquad \text{(carrier)} \tag{4}$$

Correspondence: L.W. Yousef, Dept. of Biology, School of Natural Sciences, California State University, Fresno, CA 93740-0073, U.S.A.

where P_o is the limiting permeability as C_{in} and C_o approach zero, and the K's are combinations of kinetic constants defining each of the transport steps [5–8]. (K_o and K_{in} are the half-saturation constants for zero-trans influx and efflux, respectively; K_3 is the half-saturation constant for equilibrium exchange, and K_4 is related to the mobility of the free carrier.) In addition to the above, the principle of microscopic reversibility requires that

$$\frac{1}{K_{in}} + \frac{1}{K_o} = \frac{1}{K_3} + \frac{1}{K_4} \tag{5}$$

Eqns. 2, 3, and 4 show that distinctions among the three different modes of transport can be obtained by plotting the reciprocal of the permeability against solute concentration. Simple diffusion results in a constant P, as indicated by the horizontal line of the plot. A pore will yield a straight line (with positive slope); and the carrier should show an upward curvature imparted by the quadratic term $C_{in}C_o/K_3K_4$. Our objective is to exploit these differences, and in the experiments described below, we have simplified the procedure and analysis by using small perturbations so that inside and outside penetrant concentrations are almost equal and will hereafter be denoted by C.

$$C \equiv C_o \approx C_{in} \tag{6}$$

Using Eqn. 6, our criteria Eqns. 2, 3, and 4 can be written as:

$$\frac{1}{P} = \frac{1}{P_o} = \text{constant} \qquad \text{(diffusion)} \tag{7}$$

$$\frac{1}{P} = \frac{1}{P_o} + \frac{1}{P_o}\left[\frac{1}{K_{in}} + \frac{1}{K_o}\right]C \qquad \text{(pore)} \tag{8}$$

$$\frac{1}{P} = \frac{1}{P_o} + \frac{1}{P_o}\left[\frac{1}{K_{in}} + \frac{1}{K_o}\right]C + \frac{1}{P_o}\left[\frac{1}{K_3K_4}\right]C^2 \qquad \text{(carrier)} \tag{9}$$

Determination of permeability coefficients

(a) The perturbation method. The perturbation method can be used to calculate transport parameters from the time course of a small volume change which results when salt tonicity and/or penetrant concentration around cells is rapidly altered in a specific way. These transport parameters are: P_f, the osmotic (filtration) water permeability coefficient, σ, the reflection coefficient, and P, the solute permeability coefficient.

In the absence of penetrant, a small change in external salt tonicity will result in an exponential volume change [9]. The time constant, T_w, can be used to calculate the osmotic water coefficient as follows:

$$P_f = \frac{(1-b)V_i}{T_w C_i A \bar{v}_w}\left(\frac{C_i}{C_m}\right)^2 \tag{10}$$

V_i is the isotonic volume ($79 \cdot 10^{-12}$ cm^3 at pH of 7.8 and 300 mosM, and $89 \cdot 10^{-12}$ cm^3 at pH 7.0 and 300 mosM for human erythrocytes [2]); A is the cell area ($1.42 \cdot 10^{-6}$ cm^2 for human red cells); b is the fraction of isotonic cell volume which is osmotically inactive (0.43 for human red cells, [9]); C_i is the isotonic salt concentration is osmol/cm^3; C_m is the external salt concentration in osmol/cm^3, and $\bar{v}_w$ is the partial molar volume of water (cm^3/mol).

In the presence of penetrant, any random, small perturbation of external solution will result in a volume change which can be described by the sum of two exponentials [4,10]. The time constants, T_+ and T_-, are dependent on experimental conditions and transport parameters. Measurement of the time constants can be made more accurate by choosing experimental conditions which favor one or the other. From these time constant determinations, the reflection coefficient and the permeability coefficient can be calculated at each penetrant concentration, on the assumption that the osmotic water coefficient is constant and independent of penetrant concentration.

Single exponentials from which T_+ and T_- could be determined were relatively easy to obtain for slow penetrants. However, for rapid penetrants like urea, T_- was too rapid to measure, but T_+ was very easy to measure. Assuming both the osmotic water coefficient and the reflection coefficient were constant, we calculated the permeability coefficient at each penetrant concentration from the following equation:

$$P = \frac{P_f \bar{v}_w C_m \left(\frac{T_w}{T_+}\right)\left(1 - \frac{T_w}{T_+} + \sigma^2\gamma\frac{C}{C_m}\right)}{\left(1 - \frac{T_w}{T_+}\right)\gamma} \tag{11}$$

where

$$\gamma = \left[1 + \frac{(b-a)C_m}{(1-b)C_i}\right]^{-1} \tag{12}$$

Here, a is the fraction of the isotonic cell volume which is not water. ($a = 0.3$ for human erythrocytes [11]), with other terms as defined above. Calculations of P were made using a range of reasonable values for σ (between 0.7 and 1.0). Although the particular value chosen has some effect on the magnitude of P, the linearity of the plots was unaffected.

(b) Apparatus used to monitor volume change. Two photometric devices were used to follow cell volume changes which resulted from a disturbance in the external solution. Both devices measured changes in turbidity. These turbidity changes were assumed to be directly related to changes in cell volume; refractive index corrections due to changes in internal penetrant concentra-

tion over the time course of the volume change [12] are very unlikely to be necessary since the changes in penetrant concentration within the whole cell volume, or the scatter surface, were usually very small. For example, the internal urea concentration within the scatter surface changed 25 mM or less over the course of the volume changes for experiments done on five different batches of blood (a total of 33 data points). Results on another blood batch obtained from perturbations in which urea concentration within the scatter surface changed 17 mM at the lowest urea concentration to 66 mM at the highest concentration were not different from those in which internal urea concentrations changed less. And, all these concentration changes are maximal since at least the first 250 ms were not used in the time constant calculations.

The first apparatus was described previously [9]. In this apparatus, the cell suspension (hematocrit = 1.4%) in the appropriate incubation solution was placed in a cuvette on a magnetic stirrer. Turbidity changes were recorded when the desired injection solution was introduced through a shower-head nozzle. In the second apparatus, mixing was accomplished by aspiration. A vacuum pump pulled equal volumes of cell suspension (hematocrit = 3.0%) in incubation solution and of injection solution through a Tee mixer into an observation tube placed between a red-sensitive phototube and a white light source. The turbidity changes were observed after the flow was stopped with a toggle valve.

(c) Determination of time constants from turbidity data. For each penetrant concentration, 10 to 15 perturbations were recorded and summed. A computer program fit the data to an exponential by a non-linear, least-squares iterative process. Goodness of fit was checked by comparing the curve generated from the fit parameters with the actual data. Fig. 1 shows typical data obtained from the two apparatuses with the smooth curve generated from the fit parameters. The T_+/T_∞ data were used to calculate P according to Eqns. 11 and 12.

(d) Comparison of the photometric apparatuses. Table I illustrates that the two apparatus were essentially equivalent; agreement was within 10%

(e) Experimental procedures. Human blood was obtained by venipuncture, with heparin as anticoagulant. The blood was stored at 4°C and used for experiments within five days, and usually three days, after being collected. The isotonic concentration was measured on a sample of plasma from each blood batch with a freezing point depression osmometer. Whole blood was added to the appropriate incubation solution. Both the injection and incubation solutions contained NaCl-phosphate buffer (3.7 mM KH_2PO_4 and 9.6 mM Na_2HPO_4, then adjusted to give pH of 7.0 to 7.8) and the desired concentration of penetrant. For all experiments, the temperature was about 25°C and the final constant

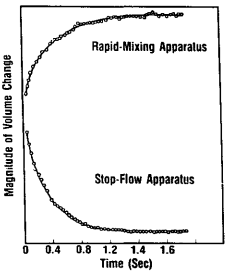

Fig. 1. Computerized fits of data superimposed on digitized volume change data. The circles are data summed from 15 osmotic swelling perturbations from the rapid-mixing apparatus (upper curve) and the stop-flow apparatus (lower curve). The smooth lines are drawn from the computer-generated exponential fits of the data. For both, cells, incubated in 298 mosM NaCl-phosphate buffer (pH 7.0), were mixed with solutions which brought the tonicity to 268 mosM. The upper curve obtained from the rapid-mixing apparatus gives a time constant of 0.47 s (P_f = 0.017 cm/s) and the lower one obtained from the stop-flow apparatus gives a time constant of 0.43 s (P_f = 0.019 cm/s). Computer fits of data in the presence of penetrants were comparable to these fits.

value of C_m/C_i varied from experiment to experiment. but was always within a range of 0.90 to 0.96. The incubation and final salt tonicities caused a maximal volume change of 10% or less.

Bovine blood, obtained from a local slaughterhouse, was defibrinated by slow stirring. Perturbation experiments were done with the cells in LeFevre's solution which contained 5.4 mM KCl, 2.6 mM $CaCl_2$, 1.8 mM $MgCl_2$, and 32 mM Tris (pH 7.4) and NaCl to give the desired tonicity.

TABLE I

Comparison between rapid-mixing and stop-flow apparatuses

Time constant measurements were made on both apparatus on the same day with the same blood (C_i = 288 mosM). For both, cells were incubated in 235 mosM NaCl (pH 7.0) plus urea and were mixed with a solution which resulted in 268 mosM NaCl-phosphate buffer and a final urea concentration from 4 to 10 mM less than was in the incubation solution. T_∞, measured in the absence of penetrant on the rapid-mixing apparatus, was 0.53 s (P_f = 0.015 cm/s) and T_∞, measured on the stop-flow appartus, was 0.60 s (P_f = 0.014 cm/s). Permeability coefficients were calculated from Eqns. 11 and 12 with the reflection coefficient assumed to be 0.95 and constant.

Final urea concn. (mM)	Rapid-mixing apparatus		Stop-flow apparatus	
	T_+ (s)	$P(\times 10^4)$ (cm/s)	T_+ (s)	$P(\times 10^4)$ (cm/s)
134	0.58	4.27	0.65	4.41
268	0.66	3.37	0.73	3.49
402	0.75	2.98	0.82	3.10

Results

Permeabilities of model penetrants diethylene glycol and glucose in human erythrocytes

Diethylene glycol was chosen as a penetrant since it plausibly penetrates by simple diffusion. Fig. 2 is consistent with this notion, i.e, the permeability coefficients for diethylene glycol were essentially independent of penetrant concentration both for swelling and shrinking within the range of concentrations used (0.2 to 1.8 M). The average P(swelling) was $8.2 \cdot 10^{-6}$ cm/s (S.E. = $0.3 \cdot 10^{-6}$, $n = 8$) over a concentration range of 130 mM to 1810 mM, and the average P(shrinking) was $7.1 \cdot 10^{-6}$ cm/s (S.E. = $0.2 \cdot 10^{-6}$, $n = 8$) over a concentration range of 134 mM to 1780 mM. (The reflection coefficient was assumed to be 1.0.) These values are not far from the P(swelling) of $6.3 \cdot 10^{-6}$ cm/s obtained by Naccache and Sha'afi [13]. This permeability is some 50-times lower than the maximum permeability observed for ethylene glycol which is presumably transported by a facilitated system [3]. The small difference between P(swelling) and P(shrinking) does not seem to be due to water rectification, since, in these cells, none was observed. A P(swelling) greater than P(shrinking) was also observed for urea.

Fig. 3 shows that a plot of the inverse of glucose permeability coefficients in 1-day-old human red cells versus concentration is nonlinear as expected. Permeabilities for all but the first two data points were calculated from Eqns. 11 and 12 with a reflection coefficient of 1. At the two lowest concentrations which were near the K values, the changing glucose concentration which occurred during the perturbation results in a range of permeabilities. This range was estimated as follows.

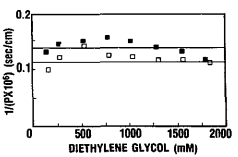

Fig. 2. Inverse permeability versus diethylene glycol concentration. Cells incubated in 247 mosM NaCl-phosphate buffer (pH 7.8) and diethylene glycol shrunk (■) after being mixed in the rapid-mixing apparatus with a solution which resulted in an external salt tonicity of 268 mosM and external diethylene glycol concentration which was 14 mM to 20 mM less concentrated than in the incubation solution. External diethylene glycol concentrations after mixing are plotted. Swelling (□) resulted when cells incubated in 295 mosM NaCl-phosphate buffer (pH 7.8) and diethylene glycol were mixed with a solution which resulted in an external salt tonicity of 268 mosM and external diethylene glycol which was 28 mM more concentrated than in the incubation solution. Horizontal lines show average permeabilities for shrinking and swelling.

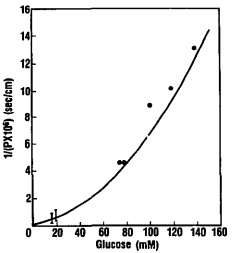

Fig. 3. Inverse permeability versus glucose concentration. Cells incubated in 296 mosM solution at pH = 7.4 were rapidly mixed in the rapid-mixing apparatus with a solution which resulted in an external salt osmolarity of 267 mosM and external glucose of 16 mM to 30 mM more than was in the incubation solution. External glucose concentrations after mixing are plotted. The solid line was drawn using transport parameters of Brahm [14].

Volume versus time data were generated from a fourth-order Runge-Kutta integration of the Kedem-Katchalsky equations with the permeability coefficient from

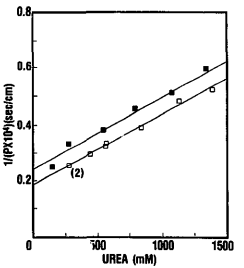

Fig. 4. Inverse permeability versus urea concentration in human erythrocytes. □ designates data collected from cell shrinkage at pH of 7.8 on the rapid-mixing apparatus; the (2) designates two identical data points. Cells incubated in 245 mosM NaCl-phosphate buffer (pH = 7.8) were mixed with a solution which resulted in a final salt tonicity of 278 mosM and external urea 3 mM to 52 mM less concentrated than was in the incubation solution. With the reflection coefficient of 0.95 [12], a linear least-squares fit of the data (correlation coefficient = 1.0) gives $V_{max} = 4.0 \cdot 10^{-4}$ mmol·cm^{-2}·s^{-1} and $K_3 = 769$ mM. ■ designates data obtained from cell shrinkage on the slop-flow apparatus with cells in pH 7.0 solution. Cells, incubated in 236 mosM NaCl-phosphate buffer (pH = 7.0) plus urea, were mixed with another solution to give an external salt tonicity of 265 mosM and external urea which was 6 to 34 mM less concentrated than was in the incubation solution. A linear least-squares fit of the data (correlation coefficient = 0.99) gave $V_{max} = 3.7 \cdot 10^{-4}$ mmol·cm^{-2}·s^{-1} and $K_3 = 866$ mM.

Eqn. 4. All K values were assumed to be 8 mM [14] and the P_o was adjusted until the time constant from the generated data matched the measured time constant. The range of permeabilities which occurred during the course of the perturbation were then calculated from Eqn. 4.

The measured glucose permeability coefficients are quite compatible with transport parameters determined by Brahm [14] as shown by the solid line in Fig. 3 (calculated with P_o of $2.75 \cdot 10^{-5}$ cm/s and all K values of 8 mM). Assuming the K values are all 8 mM, we calculated a range of P_o values from $1.4 \cdot 10^{-5}$ cm/s to $2.7 \cdot 10^{-5}$ cm/s from the measured permeability coefficients.

Thus, the perturbation method can distinguish between simple diffusion and simple carrier kinetics. Unfortunately, no model non-electrolyte penetrant is available to test the simple pore.

Permeabilities of urea, methylurea, and dimethylurea in human red cells

Fig. 4 shows the inverse urea permeability plot for human red cells in solutions of pH 7.8 and 7.0 with an assumed reflection coefficient of 0.95 [12]. Fig. 5 shows data for methylurea (with human red cells in solutions of pH 7.0) and for dimethylurea (with human cells in solutions of pH 7.0 and 7.4). We assumed a reflection coefficient of 1.0 for both methylurea and dimethylurea.

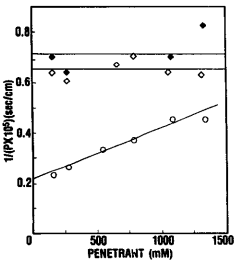

Fig. 5. Inverse permeability of human red cells versus methylurea at pH 7.0 (○) and dimethylurea at pH 7.4 (◇) and at pH 7.0 (◆). For methylurea, cells incubated in 240 mosM NaCl-phosphate buffer (pH 7.0) were mixed in the stop-flow apparatus with a solution which gave a final 270 mosM tonicity. The methylurea gradient across the red cell membranes varied from 27 to 35 mM, being more concentrated inside the cells at time zero. With a reflection coefficient of 1, a linear least-squares fit (correlation coefficient = 0.98) gave a V_{max} of $5.2 \cdot 10^{-5}$ mmol·cm^{-2}·s^{-1} and a K_3 of 1110 mM. For dimethylurea at pH = 7.4, cells incubated in 236 to 214 mosM NaCl-phosphate buffer (pH 7.4) were mixed in the rapid-mixing apparatus with a solution to give a final salt tonicity of 260 to 236 mosM; the dimethylurea was 19 to 25 mM more concentrated in the incubation solution. The average permeability coefficient was $1.5 \cdot 10^{-5}$ cm/s (S.E. = $0.1 \cdot 10^{-5}$, $n = 6$). At pH 7.0, cells incubated in 240 mosM NaCl-phosphate buffer were mixed in the stop-flow apparatus with a solution which resulted in a final salt tonicity of 270 mosM; the dimethylurea was 29 mM more concentrated in the incubation solution. The average permeability coefficient was $1.4 \cdot 10^{-5}$ cm/s (S.E. = $0.1 \cdot 10^{-5}$, $n = 4$).

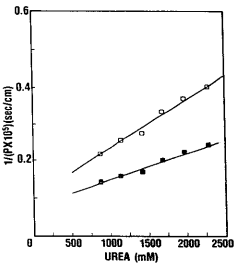

Fig. 6. Inverse permeability versus urea concentration for bovine red cells, reflection coefficient of 1.0 (■) and 0.73 (□). Bovine cells incubated in LeFevre's solution (pH = 7.4, tonicity from 307 to 287 mosM) swelled when mixed in the rapid-mixing apparatus with a solution which resulted in a final salt tonicity of 272 to 254 mosM. External urea was 49 mM more concentrated than in the incubation solution. With the reflection coefficient of 0.73 [4], a least-squares fit of the data gives V_{max} of $7.2 \cdot 10^{-5}$ mmol·cm^{-2}·s^{-1} and K_3 of 676 mM. A reflection coefficient of 1.0 results in a $V_{max} = 1.4 \cdot 10^{-4}$ mmol·cm^{-2}·s^{-1}) and $K_3 = 1090$ mM. For both fits, the correlation coefficients were 0.99.

Permeability of urea in bovine red cells

Fig. 6 shows the inverse permeability plot for bovine red cells in solutions of pH 7.4. To calculate permeability coefficients in bovine cells, it was assumed that the non-osmotic fraction of isotonic volume was 0.42, the non-solute fraction of isotonic volume was 0.24, the area per red cell was $88 \cdot 10^{-8}$ cm^2, and the isotonic cell volume was $48 \cdot 10^{-12}$ cm^3 [4]. Permeabilities were calculated for a reflection coefficient of 0.73 [4] and of 1.0.

Discussion

Urea transport in human and bovine erythrocytes is compatible with simple pore kinetics

The form of the $1/P$ versus urea concentration plots for both human and bovine red cells is compatible with simple pore kinetics, or with a simple carrier which has a very large K_4 (i.e., the lack of curvature in the plots could have been due to the limitations in the range of C). These plots are in contrast to that of diethylene glycol which follows simple diffusion and glucose which is most compatible with simple carrier kinetics.

Further discussion will be expedited by the following general transport expressions which are derived in detail in reference [8]. In these equations, we use the superscript 'p' to designate fluxes which apply to pores and superscript 'c' to refer to carriers.

For a simple carrier, the net flux is given by:

$$J^c = \frac{P_o}{1+\frac{C_o}{K_o}+\frac{C_{in}}{K_{in}}+\frac{C_oC_{in}}{K_3K_4}}(C_o - C_{in}) \tag{13}$$

while the unidirectional (efflux in this case) is given by:

$$J^c_{efflux} = \frac{P_o\left(1+\frac{C_o}{K_4}\right)C_{in}}{1+\frac{C_o}{K_o}+\frac{C_{in}}{K_{in}}+\frac{C_oC_{in}}{K_3K_4}} \tag{14}$$

Corresponding expressions for the simple pore are

$$J^p = \frac{P_o}{1+\frac{C_o}{K_o}+\frac{C_{in}}{K_{in}}}(C_o - C_{in}) \tag{15}$$

and

$$J^p_{efflux} = \frac{P_oC_{in}}{1+\frac{C_o}{K_o}+\frac{C_{in}}{K_{in}}} \tag{16}$$

(a) V_{max} for human erythrocytes agrees with literature values obtained from isotopic equilibrium exchange. The following argument shows that there are no formal kinetic differences between equilibrium exchange for a simple pore or simple carrier. For a simple pore, the unidirectional flux J_{eq} at equilibrium is obtained from Eqn. 16 by setting $C_{in} = C_o = C$. The result is

$$J^p_{eq} = \frac{P_oC}{1+\left(\frac{1}{K_{in}}+\frac{1}{K_o}\right)C} = \frac{V_{max}C}{K_{1/2}+C} \tag{17}$$

where $1/K_{1/2} = (1/K_{in} + 1/K_o)$. $K_{1/2}$ is the concentration for half-maximal velocity and $V_{max} = K_{1/2}P_o$.

The corresponding expression for a simple carrier is obtained from Eqn. 14 again by setting $C_o = C_{in} = C$ and by using Eqn. 5 together with the identity

$$1+(1/K_3+1/K_4)C+C^2/K_3K_4 = (1+C/K_3)(1+C/K_4) \tag{18}$$

We arrive at

$$J^c_{eq} = \frac{P_oC}{1+\frac{C}{K_3}} = \frac{V_{max}C}{K_{1/2}+C} \tag{19}$$

Comparison of the right hand sides of Eqns. 17 and 19 shows no formal kinetic differences. In either case, $V_{max} = K_{1/2}P_o$, but for the carrier, $K_{1/2} = K_3$. This formal distinction, i.e. for the pore, $1/K_{1/2} = 1/K_{in} + 1/K_o$ and for the carrier, $K_{1/2} = K_3$, loses its significance if, as we argue below, $1/K_4 \ll 1/K_3$. For in this case, Eqn. 5 shows that, for the carrier, $1/K_3 = 1/K_o + 1/K_{in}$, and Eqns. 17 and 19 become identical.

For urea transport, it is apparent from either Eqn. 8 (pore) or Eqn. 9 (carrier), that the value of the slope of the straight line plot of Fig. 4 gives an estimate of the reciprocal of the V_{max} to be anticipated in equilibrium exchange studies, i.e.

$$\text{slope} = (1/P_o)(1/K_{in}+1/K_o) = 1/(P_oK_{1/2}) = 1/V_{max} \tag{20}$$

Accordingly, the slopes calculated from the linear least-squares fits (correlation coefficients ranged from 0.97 to 1.0) of the urea data at pH 7.8 obtained from four different blood donors give an average V_{max} of $3.1 \cdot 10^{-4}$ mmol $\cdot$ cm$^{-2} \cdot$ s^{-1} (S.E. = $0.5 \cdot 10^{-7}$). The range from $1.8 \cdot 10^{-4}$ mmol $\cdot$ cm$^{-2} \cdot$ s^{-1} to $4.1 \cdot 10^{-4}$ mmol $\cdot$ cm$^{-2} \cdot$ s^{-1} illustrates the individual variability to which Brahm [2] alluded. These values agree with Mayrand and Levitt's value of $2.5 \cdot 10^{-4}$ mmol $\cdot$ cm$^{-2} \cdot$ s^{-1} obtained under equilibrium conditions at pH 7.28 [3], and are somewhat higher than Brahm's value of $8.2 \cdot 10^{-5}$ mmol $\cdot$ cm$^{-2} \cdot$ s^{-1}, also obtained under equilibrium exchange conditions at pH 7.2 [2]. Data obtained at pH 7.0 from two other donors gave one $V_{max} = 3.7 \cdot 10^{-4}$ mmol $\cdot$ cm$^{-2} \cdot$ s^{-1} (correlation coefficient of 1.00) and another $V_{max} = 3.2 \cdot 10^{-4}$ mmol $\cdot$ cm$^{-2} \cdot$ s^{-1} (correlation coefficient of 0.99) which corroborated Brahm's [2] finding that urea transport is relatively independent of pH in this range.

(b) Graphical estimates of $K_{1/2}$ are sensitive to small errors. Calculation of the half-saturation constant from the intercepts gives a higher value than expected, i.e., 685 mM (S.E. = 41 mM, $n = 4$) at pH 7.8, and 866 mM and 773 mM for two different blood batches at pH 7.0. Brahm [2] measured 334 mM (pH = 7.2) and Mayrand and Levitt [3] obtained 218 mM (pH = 7.28) with isotope equilibrium exchange. This difference cannot be attributed to refractive index artifacts during urea permeation [12] since the change in refractive index is negligible when internal urea concentration changes are as small as those used here. The high value may be due to the insensitivity of the method when permeability coefficients are large; for example, if time constants decrease 3% at the lowest urea concentration used, the calculated permeability coefficient changes 2-fold. In fact, time constants calculated from V_{max} of $3.3 \cdot 10^{-4}$ mmol $\cdot$ cm$^{-2} \cdot$ s^{-1} and $K_{1/2}$ of 370 mM are within 10% of those measured. Also literature values for P_o [2,3], give intercepts which are from 0.086 to 0.407. Our values ranged from 0.17 to 0.33.

(c) The urea transport data are difficult to interpret with a simple carrier; lack of curvature in the 1/P plots

implies $K_4 > 1000$ mM for human erythrocytes. If urea is transported by a simple carrier, then the lack of curvature found in Fig. 4 could only come about if the quadratic term in Eqn. 9 is negligible, i.e.

$$\frac{C}{K_3 K_4} \ll \frac{1}{K_{in}} + \frac{1}{K_o} = \frac{1}{K_3} + \frac{1}{K_4} \tag{21}$$

Substituting $K_{1/2} = K_3$, and solving for K_4

$$K_4 \gg C - K_{1/2} \tag{22}$$

Using values of $K_{1/2}$ ranging from 200 mM to 400 mM, together with the highest urea concentration used in these studies (i.e. 1853 mM), it is apparent that $K_4 \gg$ 1000 mM.

This result appears to be inconsistent with the 'qualitative estimates' of transport parameters calculated by Levitt and Mlekoday [12] assuming simple carrier kinetics: i.e., $K_{in} = 117$ mM, $K_o = 508$ mM, $K_3 = 218$ mM and $K_4 = 169$ mM. Using these values and $P_o = 1.16 \cdot 10^{-3}$ cm/s [3], we calculated the permeability coefficients and time constants we would expect at the urea concentrations we used; the $1/P$ versus urea concentration would have been highly non-linear and the time constants at the higher urea concentrations would have been much longer than those we measured. For example, at 1400 mM urea, the longest time constant we measured was 2.0 s, and the predicted time constant is 11.9 s. Clearly, our data are not consistent with the transport parameters of Levitt and Mlekoday. It must be concluded that K_4 is much larger than 169 mM as indicated in Eqn. 22.

(d) Urea efflux shows trans inhibition in human erythrocytes. Trans inhibition of urea efflux has been directly demonstrated by Frohlich and Trammel [15]. Inspection of Eqn. 16 shows that efflux trans inhibition will occur in a simple pore whenever $1/K_o \neq 0$. For a carrier, either trans acceleration or trans inhibition is possible. A criterion for trans inhibition is that $K_{in} > K_3$ [7]. To our knowledge, trans inhibition has never been found for other carrier systems in human erythrocytes. (The carrier systems most studied, i.e. glucose, leucine, uridine and choline, all show trans acceleration [7].) The glucose transport system in rabbit erythrocytes is an exception and shows neither inhibition nor acceleration due to its symmetrical nature [5].

The same conclusions are apparent in results of Brahm [2] who measured urea efflux for equilibrium exchange and for zero-trans efflux at three urea concentrations, i.e., 1 mM, 100 mM and 500 mM. The equilibrium efflux/zero-trans efflux ratio for urea calculated from these data ranges from 0.99 at 1 mM to 0.33 or 0.39 at 500 mM. Using Eqn. 19 for J_{eq} and setting $C_o = 0$ in Eqn. 13 to calculate the zero-trans flux J_{ot} we see that this ratio for the simple carrier is given by:

$$\frac{J_{eq}^{c}}{J_{ot}^{c}} = \frac{1 + \frac{C}{K_{in}}}{1 + \frac{C}{K_3}} \tag{23}$$

The corresponding equation for the simple pore is:

$$\frac{J_{eq}^{p}}{J_{ot}^{p}} = \frac{1 + \frac{C}{K_{in}}}{1 + \left(\frac{1}{K_{in}} + \frac{1}{K_o}\right) C} \tag{24}$$

Thus, Brahm's data are compatible with a pore, which must have a ratio less than one, but do not rule out a carrier, the ratio of which can be less than, equal to, or greater than one.

Methylurea transport data follow pore kinetics in human erythrocytes

No published detailed studies have been done on methylurea. Using swelling data, Naccache and Sha'afi [13] found that the methylurea permeability coefficient was $1.83 \cdot 10^{-5}$ cm/s at pH 7.2 and 277 mM penetrant. This value was 8% of their urea permeability. At the same concentration, our methylurea permeability coefficient was $3.23 \cdot 10^{-5}$ cm/s calculated from shrinking data and is 9% of the urea permeability we measured. The $1/P$ versus penetrant concentration plot (Fig. 5) fits simple pore kinetics better than simple carrier kinetics.

N,N-Dimethylurea data follow simple diffusion in human erythrocytes

N,N-Dimethylurea permeability shows little or no dependence on penetrant concentration (Fig. 5). Thus, dimethylurea could be penetrating primarily through the lipid bilayer. Mayrand and Levitt [3] measured an inhibition constant for *N,N*-dimethylurea on urea transport of 0.3 mM, while the inhibition constant for methylurea was 100 mM. Thus, the second methyl group greatly increases the binding affinity, perhaps to such an extent that little of the *N,N*-dimethylurea is actually transported by the transport system. This idea is consistent with phloretin's inability to inhibit this penetrant [17].

Can water use the urea channel?

The existence of a pore which binds and transports urea raises the possibility that water is also transported through this channel. This is a difficult issue to resolve by solute drag measurements, because conclusions based on solute drag are very sensitive to small errors in assignment of solvent flow. Resolution by osmotic flow

measurements of reflection coefficients are also equivocal. If, for example, there are two sets of channels – (1) an exclusive water pore, present in large numbers, and (2) a sparse number of urea channels that also transport water – then the osmotic effects of urea channels would be swamped by the water channels.

Conclusion

Urea and methylurea data presented here are easily explained in terms of a simple pore (channel). It is the simplest explanation and there is no necessity to propose a carrier. The notion of a simple channel for urea transport is also supported by recent data of Frohlich et al. which estimates a turnover of the order of 10^7/s (personal communication).

Acknowledgments

This study was supported by NIH Grants GM-18819 and HL-37593.

References

1 Wadzinski, L. (1974) Ph.D. Thesis U.C. Berkeley.
2 Brahm, J. (1983) J. Gen. Physiol. 82, 1–23.
3 Mayrand, R.R. and Levitt, D.G. (1983) J. Gen. Physiol. 81, 221–237.
4 Farmer, R.E.L. and Macey, R.I. (1972) Biochim. Biophys. Acta 290, 290–299.
5 Lieb, W.R. (1982) in Red Cell Membranes - A Methodological Approach (Ellory, J.C. and Young, J.D., eds.), pp. 135–164, Academic Press, New York.
6 Stein, W.D. (1986) in Transport and Diffusion Across Cell Membranes, pp. 158–173, Academic Press, New York.
7 Stein, W.D. (1986) in Transport and Diffusion Across Cell Membranes, pp. 237–242, Academic Press, New York.
8 Macey, R.I. (1986) in Physiology of Membrane Disorders, 2nd Edn. (Andreoli, T.E., Hoffman, J.F., Fanestil, D.D. and Schultz, S.G., eds.), pp. 111–131, Plenum Medical Book Company, New York.
9 Farmer, R.E.L. and Macey, R.I. (1970) Biochim. Biophys. Acta 196, 53–65.
10 Farmer, R.E.L. and Macey, R.I. (1972) Biochim. Biophys. Acta 255, 502–516.
11 Savitz, D., Sidel, V.W. and Solomon, A.K. (1964) J. Gen. Physiol. 48, 79–94.
12 Levitt, D.G. and Mlekoday, H.J. (1983) J. Gen. Physiol. 81, 239–253.
13 Naccache, P. and Sha'afi, R.I. (1973) J. Gen. Physiol. 62, 714–736.
14 Brahm, J. (1983) J. Physiol. 339, 339–354.
15 Frohlich, O. and Trammel, D. (1987) Biophys. J. 51, 514a.
16 Regen, D.M. and Morgan, H.E. (1964) Biochim. Biophys. Acta 79, 151–166.
17 Macey, R.I. and Farmer, R.E.L. (1970) Biochim. Biophys. Acta 211, 104–106.